

High-energy follow-up studies of gravitational wave transient events

Barbara Patricelli*

Università di Pisa & INFN - Pisa

E-mail: barbara.patricelli@pi.infn.it

Massimiliano Razzano

Università di Pisa & INFN - Pisa

E-mail: massimiliano.razzano@pi.infn.it

Giancarlo Cella

INFN - Pisa

E-mail: giancarlo.cella@pi.infn.it

Marica Branchesi

Università di Urbino & INFN - Firenze

E-mail: marica.branchesi@uniurb.it

Francesco Fidecaro

Università di Pisa & INFN - Pisa

E-mail: francesco.fidecaro@df.unipi.it

Michela Mapelli

INAF - Osservatorio Astronomico di Padova

E-mail: michela.mapelli@oapd.inaf.it

Elena Pian

Scuola Normale Superiore di Pisa

E-mail: elena.pian@sns.it

Antonio Stamerra

INAF-Osservatorio Astronomico di Torino & Scuola Normale Superiore di Pisa

E-mail: stamerra@oato.inaf.it

Mergers of binary systems of compact objects are the most promising sources of gravitational waves (GWs) and are thought to be connected to some of the most energetic events in the universe: short Gamma Ray Bursts (GRBs). A definitive probe of this association is still missing and combined observations of gravitational and electromagnetic (EM) signals from these events are crucial to unveil the progenitors of short GRBs and study the physics of compact objects. We investigate the possibility of joint GW and EM observations of merging binary systems with the GW detectors Advanced LIGO and Advanced Virgo and with the Large Area Telescope (LAT) instrument on-board the *Fermi* γ -ray observatory.

The 34th International Cosmic Ray Conference,

30 July- 6 August, 2015

The Hague, The Netherlands

1. Introduction

The second-generation gravitational wave (GW) interferometers of the Advanced LIGO and Advanced Virgo project are currently undergoing major upgrades and will soon reach sensitivities sufficient to detect GWs directly for the first time, opening a new era in the multi-messenger investigations of the universe. One of the most promising sources for detection with Advanced LIGO and Advanced Virgo is the coalescence of binary systems of compact objects: binary neutron stars (NS-NS) and/or black holes (NS-BH, BH-BH). In fact, during the final stages of their inspiral phase, just before the merging of the two stars, these systems are very strong emitters of GWs in the frequency range covered by LIGO and Virgo (~ 10 Hz - 10 kHz). The merger of NS-NS and NS-BH systems could be also accompanied by electromagnetic (EM) emission. In particular, there are several evidences that short gamma-ray bursts (GRBs) originate from these mergers (see [1] and references therein). Short GRBs are intense flashes of γ rays lasting less than 2 seconds, sometimes accompanied by a long lasting weaker “afterglow” emission. They are thought to be powered by accretion onto the central compact object formed in the NS-NS or NS-BH system coalescence; the simultaneous detection of a short GRB and a GW signal will be a definitive proof of binary systems being the progenitors of these extremely energetic events. Furthermore, the detection of a coincident EM signal will increase the confidence of the GW detection of the merger, and provide complementary information (such as the precise sky localization or the distance to the source) on the event. Therefore, the EM follow-up of the merger of binary systems represents a key tool to better understand the physics underlying these extreme events and to unveil the nature of short GRB progenitors.

Among the various γ -ray instruments, the Large Area Telescope (LAT) on-board the *Fermi* satellite [2] is well suited for the EM follow-up of GW candidates for several reasons. First of all, its large field-of-view (FOV, ~ 2.4 sr) can cover with few tiled exposures the large error boxes associated with the GW sky localizations provided by the alerts. Moreover, it can localize accurately the sources (the on-axis, 68% containment radius at 10 GeV is 0.8 deg), and disseminate these refined locations among other observatories for the follow-up of the GW events at other wavelengths.

Here we investigate the possibility for high energy follow-up of merging binary systems with the LAT. In particular, we focus on merging NS-NS systems, whose gravitational waveform is well modeled and understood. The work is organized as follows. In Sec. 2 we explain how we generate a sample of merging NS-NS systems. In Sec. 3 we present the procedure we use to estimate the GW detection rates and sky localization of the simulated events. In Sec. 4 we describe how we simulate the GRBs associated to the mergers and compare their EM emission with the LAT sensitivity. Finally, in Sec. 5 we present our results.

2. The merging NS-NS systems

The first step to construct a distribution of realistic NS-NS merging systems detectable by Advanced Virgo and Advanced LIGO is the generation of a sample of synthetic galaxies. We

*Speaker.

[†]This work has been supported by the contract FIRB-2012-RBFR12PM1F of the Ministry of Education, University and REsearch (MIUR).

38 assume that Milky Way like galaxies dominate the Local Universe¹ and we use a constant galaxy
 39 density of 0.0116 Mpc^{-3} , that is the extrapolated density of Milky Way equivalent galaxies in
 40 space [3]. We give each galaxy a random, isotropic and uniform location in the sky and cut off
 41 the distribution at a distance of 250 Mpc, that is beyond the NS-NS range² of Advanced Virgo
 42 and Advanced LIGO in their final configuration [4]. Then we populate each galaxy with several
 43 merging NS-NS systems in accordance with the merger rate reported in [5], that we assume to have
 44 the same value for all galaxies; we consider an observing time of 1 year.

45 To populate the galaxies we extract merging NS-NS systems from a sample that we generate
 46 in the following way. We use the public synthetic database available at www.syntheticuniverse.org,
 47 developed by Dominik et al. 2012 [5]. They investigated the evolution of binary systems that leads
 48 to the formation of merging binary systems of compact objects (NS-NS, NS-BH and BH-BH) for
 49 a synthetic galaxy resembling the Milky Way. They use different population synthesis models, to
 50 account for the uncertainties associated with several evolutionary processes such as., i.e., stellar
 51 winds and consider two metallicities: $Z=Z_{\odot}$ and $Z=0.1 Z_{\odot}$, where Z_{\odot} is the solar metallicity.
 52 Here we focus on NS-NS systems with $Z=Z_{\odot}$ and generated with the so called “standard model -
 53 submodel A”; a more complete study including all other models and metallicity will be presented
 54 elsewhere.

55 For each binary system, the database provides the masses of the two compact objects, as well
 56 as an estimate of the merging time (sum of the time needed to form the two compact objects and
 57 the time for the two compact objects to coalesce). If the total time (merger time plus a randomly
 58 assigned starting time) is less than the age of the galaxy, assumed to be 10 Gyr, the system can be
 59 considered as a merging system and is included in our sample.

60 To reduce the statistical uncertainties, we generate 1000 realizations, each one for a 1 year
 61 observing period.

62 3. GW detections and sky localizations

63 We assign to each NS-NS merging system the same sky position (right ascension, declination
 64 and distance) of the host galaxy, and a random inclination of the orbital plane with respect to the
 65 line of sight. For simplicity, we assume that the systems are non-spinning.

66 For each merging NS-NS system, we simulate the expected GW inspiral signals, using the
 67 “TaylorT4” waveforms (see, e.g., [6]). After the GW signals have been simulated, we convolve
 68 them with the GW detector responses. We use the sensitivity curves of Advanced LIGO and Ad-
 69 vanced Virgo reported in [4], describing five possible observing scenarios representing the evolving
 70 configuration and capability of Advanced LIGO and Advanced Virgo. In particular, we focus on
 71 two of these scenarios: the 2016-2017 scenario and the expected final “design” configuration, that
 72 will be achieved in 2019 and 2021 by Advanced LIGO and Advanced Virgo respectively. For the
 73 “design” configuration we use the noise power spectral density (PSD) curves reported in fig. 1
 74 of [4]; for the 2016-2017 configuration we use the noise PSD curves in the middle of the ranges
 75 reported in [4].

¹In this work we neglect the contribution of elliptical galaxies and galaxy clusters; a more detailed study will be presented elsewhere.

²Location and system orientation average distance.

76 The data obtained in this way are then analyzed with the matched filtering technique [7]. With
 77 this technique the data from all detectors are Wiener filtered with an array of theoretically modeled
 78 template waveforms (a “template bank”), constructed with different choices of the intrinsic param-
 79 eters (e.g. the masses) of the binary systems. The output is an estimate of the signal to noise ratio
 80 (SNR) with respect to that template in that detector. If the signal results in a SNR above a given
 81 threshold in at least two detectors, with the same binary parameters and within approximately one
 82 light-travel time between detectors, it is considered as a GW candidate.

83 For simplicity, we construct template banks specifically designed to detect our simulated sig-
 84 nals, e.g. with the same intrinsic parameters used for the simulated signals; the waveform we use
 85 is the “TaylorF2” (see [6]). We impose a network (two or three detectors) SNR (root sum square
 86 of the individuals SNR) threshold $\rho_c=12$, that corresponds to a false alarm rate (FAR) below 10^{-2}
 87 yr^{-1} [4].

88 For each GW candidate we then estimate the associated sky localization with BAYESTAR,
 89 a rapid Bayesian position reconstruction code that produces accurate probability sky maps in less
 90 than a minute after any NS-NS merger detection: this allows the prompt delivery of alerts to the
 91 astronomical community, enabling the EM follow-up of the GW events [8]. BAYESTAR is part
 92 of the LALSuite project, that comprises the routines for the analysis of GW data developed by the
 93 LIGO scientific collaboration and the Virgo collaboration.

94 We consider two cases: an optimistic one, in which all the interferometers are operating with
 95 a 100% duty cycle and a more realistic case, in which the GW detectors have an independent 80 %
 96 duty cycle (see for example [4]).

97 4. The simulated GRB sample

98 We assume that all the mergers of NS-NS systems are followed by a short GRB. We construct
 99 the light curve and spectrum of these GRBs using GRB 090510 as a template. This choice is
 100 motivated by the fact the GRB 090510 is the only short GRB to show emission up to GeV energies
 101 and, in particular, to show an extended emission (up to 200 s) at high energies (up to 4 GeV), as
 102 detected by the LAT [9]: this is a fundamental characteristic, since the overall time required to send
 103 GW alerts (a few minutes, see e.g. [8]) will not allow to follow-up the short GRBs themselves, but
 104 only their weaker afterglow emission.

105 The spectrum of the extended emission of GRB 090510 showed no significant evolution and
 106 it is well fitted by a power law with photon index $\alpha=-2.1$ [10]; the light curve is well fitted by a
 107 power law with a decay index $\alpha_t=1.38 \pm 0.07$ [10]. We assume that the extended emission of the
 108 simulated GRBs has the same power law decay in time and the same spectral shape observed for
 109 GRB 090510. We then re-scale the observed flux of GRB 090510 to take into account the different
 110 total energy and distance of the source. In particular, we assume that the total EM energy emitted
 111 in γ rays during the prompt emission, E_γ^{prompt} is in the range observed for short GRBs, i.e. 10^{49} erg
 112 $\leq E_\gamma^{\text{prompt}} \leq 10^{53}$ erg (see e.g. [1, 9]). Then, we assume that the fraction of energy emitted in γ rays
 113 during the afterglow is the same observed by LAT for GRB 090510, i.e. $\sim 0.5 E_\gamma^{\text{prompt}}$.

114 We also correct for the different inclination angle of the binary systems θ (corresponding to
 115 the angle of the GRB jet with respect to the line of sight). To do this, we consider a simplified
 116 model of a point source moving with a constant Lorentz factor Γ (see, for example, the model 1 in

117 [11]). Here we choose $\Gamma=100$, that is a reasonable value for the early afterglow emission; a more
 118 detailed analysis with different values of Γ will be presented elsewhere.

119 To verify if such simulated GRBs could be detectable by the LAT, we estimate the total inte-
 120 gration time t_f required to have a fluence equal to the high energy LAT sensitivity corresponding
 121 to a GRB localization at $1-\sigma$ of 1 deg. This sensitivity has been estimated by extrapolating the one
 122 obtained with the Pass 7 reprocessed instrument response function of the LAT³ to the energy range
 123 0.1-300 GeV. We consider the LAT working in the survey mode.

124 5. Results

125 5.1 GW detections

126 Of the ~ 18000 simulated NS-NS merging systems, about the 7.5 % (5.4 %) and 49.4 % (37.5
 127 %) were GW detected with the 2016-2017 and design configuration respectively and considering a
 128 100 % (80 %) independent duty cycle of each interferometer. The average GW detection rates are
 129 reported in Tab. 1. For comparison, we also report the values obtained by Aasi et al. 2013 [4] and
 130 Singer et al. 2014 [8], that have been obtained considering an 80 % duty cycle: it can be seen that
 131 all the values are consistent, within the error bars; the apparent discrepancy in the number of GW
 132 detections of NS-NS systems between our value and the one reported in Singer et al. 2014 [8] is a
 133 consequence of the higher merger rate they use.

134 To give an estimate of the accuracy of the sky localization of these GW events, we calculate
 135 the expected cumulative number of detections as a function of the areas, in deg^2 , inside of the
 136 smallest 90 % confidence regions; these contours were constructed with the “water-filling” algo-
 137 rithm introduced in [8]. The results are shown in Fig. 1 and in Tab. 1. It can be seen that, with the
 138 design configuration and a 80 % duty cycle, ~ 2 events per year could be GW detected with a sky
 139 localization $\leq 20 \text{ deg}^2$, small enough to allow for the LAT follow-up.

140 5.2 Joint EM and GW detections

141 Fig. 2 and Tab. 2 show the cumulative percentage of GRBs detectable by *Fermi*-LAT, as well
 142 as the cumulative percentage of events detectable both in EM and GW, as a function of the integra-
 143 tion time t_f . It can be seen that, for an integration time of 1000 s, ~ 3.6 % (1.0 %) of the mergers
 144 can be detected both in EM and GW for $E_\gamma^{\text{prompt}} = 10^{53}$ erg (10^{49} erg) and when considering the de-
 145 sign configuration and a 100 % duty cycle of the interferometers: this corresponds to a rate of joint
 146 EM and GW detections of $\sim 0.6 \text{ yr}^{-1}$ ($\sim 0.2 \text{ yr}^{-1}$). The estimated rates of EM detections should
 147 be considered as upper limits, since we are assuming that each NS-NS merger is accompanied by
 148 a GRB with emission at high energies.

149 It is worth to recall that these estimates have been obtained considering only NS-NS systems;
 150 a more complete analysis including NS-BH systems will be presented elsewhere. The inclusion of
 151 NS-BH systems is expected to increase the EM detection rate, due to the higher number of possible
 152 GRB progenitors and the larger explorable universe, since NS-BH mergers can be detected by GW
 153 interferometers up to larger distances with respect to NS-NS systems.

³http://www.slac.stanford.edu/exp/glast/groups/canda/archive/p7rep_v15/lat_Performance.htm

Configurations	Simulations	Number of NS-NS detections (yr^{-1})	% of NS-NS Localized within 5 deg^2	% of NS-NS Localized within 20 deg^2
2016-2017	Aasi et al. 2013 [4]	0.006-20	2	5-12
	Singer et al. 2014 ^a [8]	1.5	2	8
	Sim., 80 % duty cycle	0.5 (0.01-1.7)	$2.3^{+1.2}_{-0.8}$	$7.9^{+1.9}_{-1.5}$
	Sim., 100 % duty cycle	0.7 (0.01 - 2.3)	$2.8^{+1.0}_{-0.8}$	$10.8^{+1.8}_{-1.6}$
2019+ (design)	Aasi et al. 2013 [4]	0.2-200	3-8	8-28
	Sim., 80 % duty cycle	7.5 (0.05 - 12.4)	$7.6^{+0.7}_{-0.6}$	$27.6^{+1.1}_{-1.1}$
	Sim., 100 % duty cycle	8.8 (0.05 - 14.6)	$10.8^{+0.7}_{-0.6}$	$38.5^{+1.0}_{-1.0}$

^aThese estimates refer to the 2016 scenario.

Table 1: Expected GW detection rate and source localization for the 2016-2017 and the 2019+ (design) configurations, with an independent 80% duty cycle of each interferometer, as assumed in [4] and [8]. For the 2016-2017 configuration, our estimated number of NS-NS detections has been re-scaled to a 6-months observation period, to do a direct comparison with [4] and [8]. The range of GW detection rates reported in parenthesis has been estimated considering the highest range of NS-NS merger rates reported by Dominik et al. 2012, corresponding to model V12, submodels A and B [5].

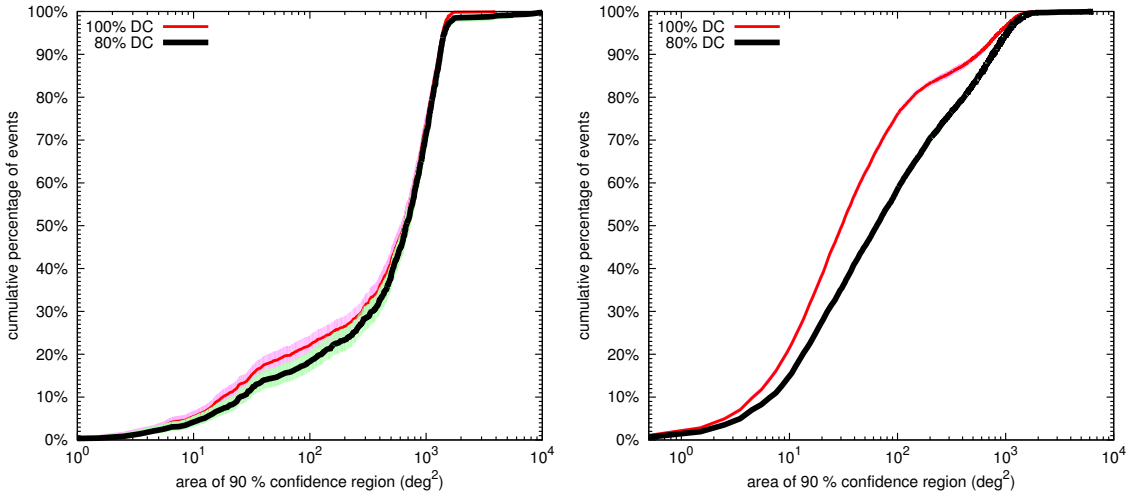


Figure 1: Cumulative histograms of sky localization areas in the 2016-2017 (left) and in the design (right) scenarios. The shadowed regions enclose the 95 % confidence intervals accounting for sampling errors, as computed from the quantiles of a beta distribution (see [12]).

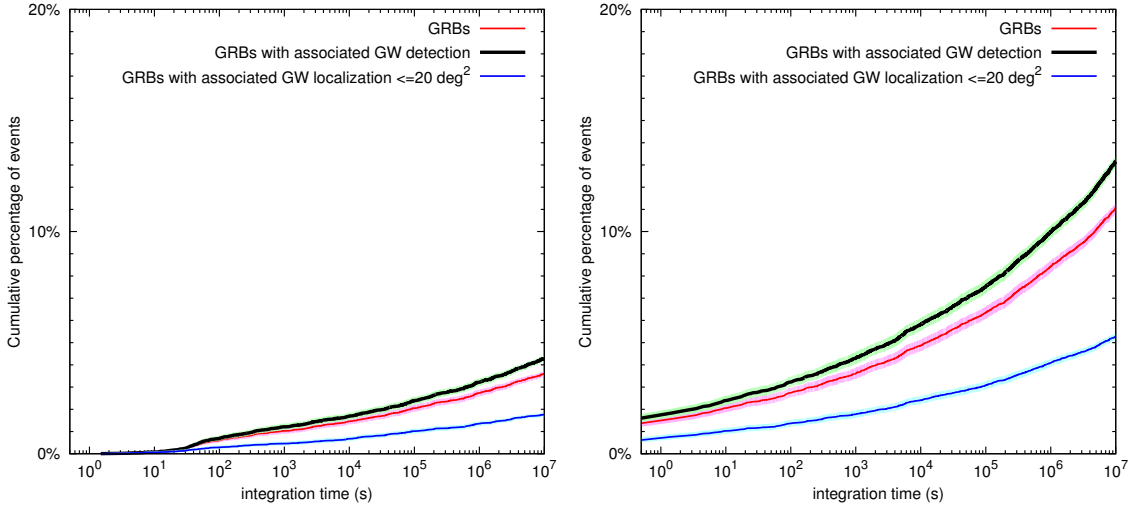


Figure 2: Left: cumulative histogram of the integration time needed for the simulated GRBs (in red), for the simulated GRBs with associated GW detection (in black) and with a sky localization $\leq 20 \text{ deg}^2$ (in blue) to be detected by the LAT. We assume $E_{\gamma}^{\text{prompt}} = 10^{49} \text{ erg}$ and, for the GW detections, we consider the design scenario and a 100 % duty cycle of each interferometer. Right: same as left, but we assume $E_{\gamma}^{\text{prompt}} = 10^{53} \text{ erg}$.

Integration Time (s)	% of GRBs with EM detection	% of GRBs with EM and GW detections	% of GRBs with EM and GW detections, with GW localization within 20 deg^2
10	2.4 (0.1)	2.1 (0.1)	1.0 (0.1)
200	3.5 (0.9)	3.0 (0.8)	1.5 (0.3)
1000	4.3 (1.2)	3.6 (1.0)	1.8 (0.5)

Table 2: Expected percentages of EM and GW detections for the 2019+ (design) configuration, considering a 100 % duty cycle of the interferometers and assuming $E_{\gamma}^{\text{prompt}} = 10^{53} \text{ erg}$ (10^{49} erg).

References

- [1] Berger, E., *Short-Duration Gamma-Ray Bursts*, ARAA **52** (2014) 43
- [2] Atwood, W.B., et al., *The Large Area Telescope on the Fermi Gamma-Ray Space Telescope Mission*, ApJ **697** (2009) 1071
- [3] Kopparapu, R.K., et al., *Host Galaxies Catalog Used in LIGO Searches for Compact Binary Coalescence Events*, ApJ **675** (2008) 1459
- [4] Aasi, J., et al., *Prospects for Localization of Gravitational Wave Transients by the Advanced LIGO and Advanced Virgo Observatories*, gr-qc/1304.0670

- 162 [5] Dominik, M., et al., *Double Compact Objects. I. The Significance of the Common Envelope on*
163 *Merger Rates*, ApJ **759** (2012) 52
- 164 [6] Buonanno, A., et al., *Comparison of post-Newtonian templates for compact binary inspiral signals in*
165 *gravitational-wave detectors*, PhRvD **80** (2009) 4043
- 166 [7] Wainstein, L.A., et al., *Extraction of signals from noise*, Prentice-Hall (1962)
- 167 [8] Singer, L. P., et al., *The First Two Years of Electromagnetic Follow-up with Advanced LIGO and*
168 *Virgo*, ApJ **795** (2014) 105
- 169 [9] Ackerman, et al., *Fermi Observations of GRB 090510: A Short-Hard Gamma-ray Burst with an*
170 *Additional, Hard Power-law Component from 10 keV To GeV Energies*, ApJ **716** (2010) 1178
- 171 [10] De Pasquale, M., et al., *Swift and Fermi Observations of the Early Afterglow of the Short Gamma-Ray*
172 *Burst 090510*, ApJ **709** (2010) 146
- 173 [11] Granot, J., et al., *Off-Axis Afterglow Emission from Jetted Gamma-Ray Bursts*, ApJ **570** (2002) 61
- 174 [12] Cameron, E., *On the Estimation of Confidence Intervals for Binomial Population Proportions in*
175 *Astronomy: The Simplicity and Superiority of the Bayesian Approach*, PASA **28** (2011) 128